

Conditioning nano-LEDs in arrays by laser-micro-annealing: The key to their performance improvement ^{EP}

Cite as: Appl. Phys. Lett. **118**, 043101 (2021); <https://doi.org/10.1063/5.0038070>

Submitted: 18 November 2020 • Accepted: 13 January 2021 • Published Online: 27 January 2021

 M. Mikulics, P. Kordoš, D. Gregušová, et al.

COLLECTIONS

 This paper was selected as an Editor's Pick



View Online



Export Citation



CrossMark

ARTICLES YOU MAY BE INTERESTED IN

[A high efficiency standalone magnetoelectric energy converter based on Terfenol-D and PZT laminate](#)

Applied Physics Letters **118**, 044101 (2021); <https://doi.org/10.1063/5.0030993>

[Imaging confined and bulk p-type/n-type carriers in \(Al,Ga\)N heterostructures with multiple quantum wells](#)

Applied Physics Letters **118**, 032104 (2021); <https://doi.org/10.1063/5.0026826>

[Development of microLED](#)

Applied Physics Letters **116**, 100502 (2020); <https://doi.org/10.1063/1.5145201>



Timing is everything.
Now it's automatic.

A new synchronous source measure system for electrical measurements of materials and devices

 **Lake Shore**
CRYOTRONICS

[Learn more](#)

Conditioning nano-LEDs in arrays by laser-micro-annealing: The key to their performance improvement

Cite as: Appl. Phys. Lett. **118**, 043101 (2021); doi: [10.1063/5.0038070](https://doi.org/10.1063/5.0038070)

Submitted: 18 November 2020 · Accepted: 13 January 2021 ·

Published Online: 27 January 2021





View Online



Export Citation



CrossMark

M. Mikulics,^{1,2,a)}  P. Kordoš,³ D. Gregušová,³ Z. Sofer,⁴ A. Winden,⁵ St. Trellenkamp,⁶ J. Moers,⁶ J. Mayer,^{1,2} and H. Hardtdegen^{1,2,a)} 

AFFILIATIONS

¹Jülich-Aachen Research Alliance, JARA, Fundamentals of Future Information Technology, D-52425 Jülich, Germany

²Ernst Ruska-Centre (ER-C-2), Forschungszentrum Jülich, D-52425 Jülich, Germany

³Institute of Electrical Engineering, Slovak Academy of Sciences, Dúbravská cesta 9, SK-84104 Bratislava, Slovak Republic

⁴Department of Inorganic Chemistry, Institute of Chemical Technology, Technická 5, Prague 6, Czech Republic

⁵Robert Bosch GmbH, D-72760 Reutlingen, Germany

⁶Helmholtz Nanoelectronic Facility (HNF), Forschungszentrum Jülich, D-52425 Jülich, Germany

^{a)}Authors to whom correspondence should be addressed: m.mikulics@fz-juelich.de and h.hardtdegen@fz-juelich.de

ABSTRACT

A local so-called laser-micro-annealing (LMA) conditioning technology, which is suitable for the fabrication of a large range of hybrid nano-optoelectronic devices, was applied to III-nitride-based nano-light emitting diodes (LEDs). The LEDs with a diameter of ~ 100 nm were fabricated in large area arrays and designed for hybrid optoelectronic applications. The LMA process was developed for the precise local conditioning of LED nano-structures. Photoluminescence measurements reveal the enhancement of nano-LED properties, which is in very good agreement with a simple model introduced based on the reduction of the defect layer depth by the LMA process. The experimental data confirm the reduction of the defect layer depth from ~ 17 nm to ~ 5 nm determined. In consequence, an increase in work currents up to 40 nA at 5 V bias after the LMA procedure as well as high electroluminescence (EL) and output optical power up to 150 nW in the ~ 440 – 445 nm emission wavelength range corresponding to $\sim 75\%$ wall-plug efficiency were achieved. Additionally, the LEDs' electroluminescence intensities reach the desired values by conditioning the contact/annealed regions of individual LEDs accordingly. Furthermore, the LMA process affects the long-term stability of the electroluminescence (EL) intensity of single nano-LED devices. A study of the EL during 5000 h in the continuous wave operation testing mode revealed a moderate $\sim 15\%$ decrease in the intensity in comparison to $\sim 50\%$ for their non-LMA counterparts. Finally, Raman measurements indicate that the “work” temperature for nano-LED conditioned structures decreases.

© 2021 Author(s). All article content, except where otherwise noted, is licensed under a Creative Commons Attribution (CC BY) license (<http://creativecommons.org/licenses/by/4.0/>). <https://doi.org/10.1063/5.0038070>

Currently, there is growing interest in the development of nano-optoelectronic devices.^{1–5} The small dimensions of such nano-structures are advantageous for obtaining a high integration density, on the one hand, and for the utilization of quantum size effects, on the other hand.⁶ Furthermore, nano-structures exhibiting different physical, chemical, optical, and electrical properties could be combined into hybrid circuits for novel devices with enhanced functionality.⁷ During the last few decades, light emitting diodes (LEDs) based on different material systems were implemented in a broad range of optoelectronic applications.^{8–10} The miniaturization of the LEDs toward micro-LEDs^{11–14} led to a wealth of additional applications¹⁵ such as in

display technology^{16,17} and sensing.¹⁸ A further size reduction toward the nano-scale^{19,20} allows applications, for example, in Li-Fi communication²¹ and/or as few photon sources.^{7,22,23} Recently, we proposed that nano-LED arrays emitting at short wavelengths down to the ultraviolet (UV) range can be used as key elements for future nano-LED-assisted lithography.²³ Group-III-nitride-based nano-LEDs arranged in arrays are the essential part of this lithographical technique. The realization of stable and reliable nano-LEDs with uniform intensity, however, is still a challenge and obstructs their broader application: on the one hand, from a materials point of view, fluctuations in the alloy composition of the InGaN/GaN multi-quantum well

structures can affect their electronic and optical properties.²⁴ On the other hand, the preparation of the nano-LEDs, for example, by etching nano-wires (NWs) from layers^{25,26} as one of the most critical steps in the nano-LED fabrication process affects their radiative recombination because of the formation of etching-induced defects. Earlier work dealt with the influence of etching parameters on the nano-LEDs' optical properties and, especially, on radiative recombination.²⁵ This Letter focuses in contrast on the local laser annealing of the nano-LEDs in arrays as an additional step after they were fabricated by the reactive ion etching (RIE) approach and subsequent device fabrication. The aim was to improve their electrical and optical parameters.

In general, the spatial and temporal control for processing and material modification using lasers as the energy sources emerged as a new field in materials science in the late 1970s. Laser annealing was employed to heal ion implantation damage^{27,28} as well as in the processing of nano-structures and the annealing of contacts to nano-wire and thin film transistor devices.^{29–31} This is in analogy to recently demonstrated post metallization annealing in the processing of group III-N-based transistors,^{32,33} which led to the reduction of electronic states at the $\text{Al}_2\text{O}_3/\text{AlGaIn}$ interface. The goal of the studies was to reduce the contact resistance and—for practical and industrial applications—to use as small as possible annealing times. In this report, we will center our attention to the effect of a so-called laser-micro-annealing (LMA) process³⁴ developed for the precise local conditioning of Ni/Au on p-GaN Ohmic contacts and the curing of etching defects in the Multi Quantum Well (MQW) region important for an increase in radiative recombination, which is essential for the improvement of the electrical and optical performance of the devices.^{35–37} It was implemented to determine the charge transport and light emission of the

nano-LEDs.³⁸ The effect of LMA on the electroluminescence (EL) intensity of the nano-LEDs was investigated and the long-term stability of their EL under the continuous wave (cw) operation testing mode was studied in comparison to non-locally conditioned nano-LED devices. We demonstrate that the local laser-micro-annealing (LMA) process and its tuning for the conditioning of individual nano-LEDs (whilst focusing on their optically transparent p-GaN Ni/Au Ohmic contact) are the key to improving their performance and to achieving stable and reliable nano-LEDs down to the tens of nm size range.

The fabrication process started with the MOVPE growth of the n-GaN, the InGaIn/GaN Multi Quantum Well (MQW), and the p-GaN LED layers in a homemade MOVPE reactor.^{39,40} Arrays of hexagonally arranged Ni caps with a diameter of 100 nm served as the etching mask and were defined using e-beam lithography. Details to the device fabrication have been described earlier.^{22,23} RIE was carried out in an Oxford Plasmalab 100 reactor with an inductively coupled plasma (ICP) 180 source at a pressure of 4 μbar , a sample temperature of 5 °C, a chlorine:argon gas mixture of 16:4, and an ICP power of 750 W [schematics in Fig. 1(a)], resulting in arrays of single nano-LED structures as depicted in Figs. 1(d) and 1(e). For electrical isolation, the etched nano-structures were buried in hydrogen silsesquioxane, which formed SiO_2 upon annealing. The nano-LEDs were integrated into a vertical device layout, which serves for their biasing and which allows for the subsequent DC electrical measurements and device operation. Details have been described earlier.^{7,23} The protruding Ni caps were removed wet-chemically in a solution of $\text{HCl:H}_2\text{O}$, and transparent Ni/Au (5/5 nm) top contacts⁴¹ were prepared using conventional optical lithography and a conventional rapid thermal annealing process.⁴² Subsequently, single nano-LEDs were conditioned locally using a

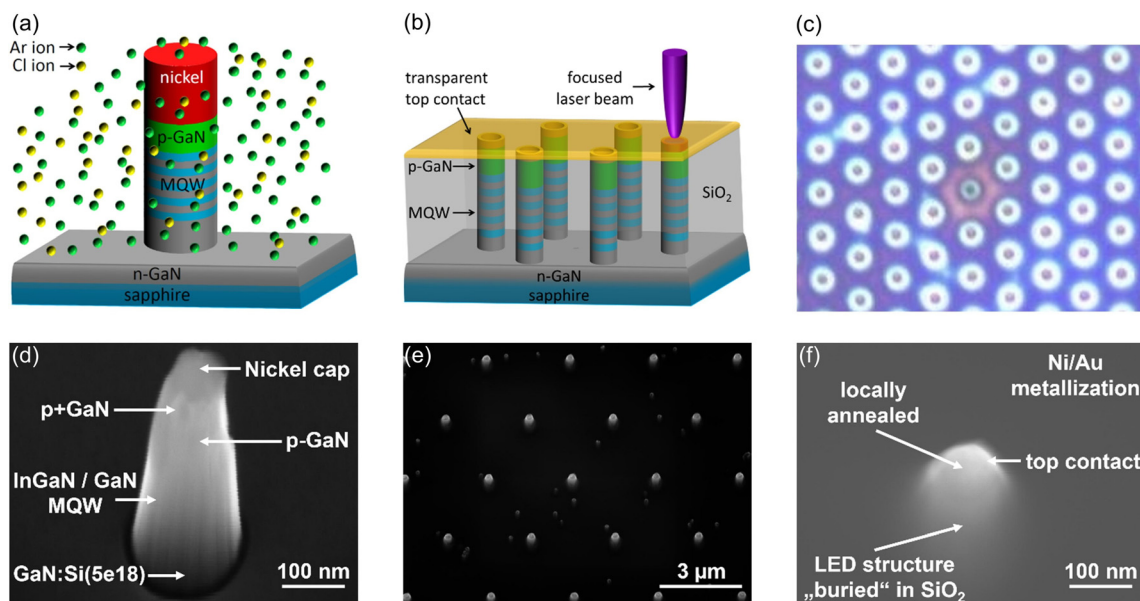


FIG. 1. (a) Fabrication schematics of the group-III nitride-based nano-LED defined with the help of the reactive ion etching (RIE) approach. A nickel cap serves as the protecting/etching mask.^{7,23,25} (b) Schematics of the so-called laser-micro-annealing (LMA) process. Precise local annealing of the nano-LEDs is carried out above the Ni/Au transparent top contact. (c) Optical micrograph of a nano-LED array with a pitch of 3 μm . A single nano-LED is annealed locally (structure centered in the middle) by the LMA process. The laser (HeCd, 325 nm) input power was kept constant at $\sim 0.8 \text{ kW/cm}^2$. Scanning electron micrographs (SEM) of (d) a single nano-LED with its nickel mask for RIE, (e) the nano-LED array, and (f) the nano-LED buried in SiO_2 with its top contact.

laser-micro-annealing process shown schematically in Fig. 1(b). The laser (HeCd, 325 nm) input power was kept constant at $\sim 0.8 \text{ kW/cm}^2$. Figure 1(c) presents an optical micrograph of the nano-LED array in which the locally conditioned nano-LED is in the center of the image and Fig. 1(f) shows the nano-LED buried in SiO_2 with its transparent Ni/Au annealed top contact.

Before the nano-LEDs were conditioned by the laser-micro-annealing process, they were first “tested” by micro-photoluminescence (micro-PL) spectroscopy at room temperature. The samples were excited with the 325 nm line of a HeCd laser.

The laser input power was kept constant at $\sim 0.1 \text{ kW/cm}^2$ to prevent any further local laser-micro-annealing. The PL spectra recorded at room temperature of LMA conditioned nano-LEDs with a diameter of $\sim 100 \text{ nm}$ [Fig. 2(a)] exhibit a large increase in luminescence intensity in the blue region of the spectra attributed to the MQWs in comparison to their non-LMA conditioned counterpart by more than a factor of two. Additionally, the intensity of the peak related to the GaN band edge luminescence and the defect luminescence at 564 nm corresponding to $\sim 2.2 \text{ eV}$ increases by $\sim 8\%$ and decreases by $\sim 9\%$, respectively. Here, it must be noted that the photon penetration depth of the 325 nm laser in GaN is on the order of 80–100 nm (Refs. 43 and 44) and since the laser excitation spot size is $\sim 0.5 \mu\text{m}$ in diameter, the measured defect luminescence has its major contribution from the etched device material surrounding the nano-LED structure. This indicates that the LMA process at least partially cures⁴⁵ etching related defects, which are responsible for the suppression of radiative recombination in the nano-LEDs. The micro-PL mapping presented in Fig. 2(b) describes graphically (in colors) the “overall” distribution from the single nano-LEDs in the array—the etching process is responsible for the suppression of radiative recombination from the MQW region: the blue color with inhomogeneous intensity corresponds to an emission wavelength of $\sim 440\text{--}445 \text{ nm}$. Furthermore, the “defect” luminescence: green–yellow and red corresponds to emission maxima in the PL spectra of $\sim 540\text{--}600 \text{ nm}$ at the individually measured points. The experimental results indicate that radiative recombination is suppressed, which is attributed to damage induced by the etching process

as was previously reported.^{7,25} A comparison between the emission from the central region of a single nano-LED before and after the annealing process [Figs. 2(c) and 2(d)] discloses that the PL intensity increases greatly upon local annealing. A model for the enhancement of nano-LED properties is discussed in the following. The etched nano-LEDs in this study were fabricated additionally from the same MQW layer (parent) structure. The nominal volume of the MQW structure can be expressed in the simple form as $V_{\text{MQW}} = \pi/4 \times d_{\text{nom}}^2 \times h$, where h is the total height/the thickness of the MQW region. In our simplified model (Fig. 3), we assume in contrast to Ryu *et al.*⁴⁶ “ideal” material for V_{MQW} . However, the effective nano-LED volume contributing to radiative recombination is smaller than V_{MQW} due to the formation of a defect layer with a depth ($\text{depth}_{\text{def}}$) induced by the etching process forming non-radiative recombination centers. Furthermore, for the sake of simplification, we introduce the virtual equivalent of the effective volume (V_{eff}), which is in analogy to V_{MQW} ; therefore, $V_{\text{eff}} = \pi/4 \times (d_{\text{nom}} - 2 \times \text{depth}_{\text{def}})^2 \times h$.

Since the respective laser excitation density was kept constant, we assume that the integrated photoluminescence intensity (I_{PL}) is related to the virtual V_{eff} and, therefore, to $(d_{\text{nom}} - 2 \times \text{depth}_{\text{def}})^2$. The integrated photoluminescence intensity (I_{PL}) normalized to the as-grown MQW (parent) structure was investigated for different nano-LED diameters (d_{nom}). The experimental data are presented in Fig. 3(b) for non-locally annealed and laser-micro-annealed nano-LEDs with different diameters. We determined values for the defect layer depth ($\text{depth}_{\text{def}}$) of $\sim 17 \text{ nm}$. This value is in the same range reported earlier.⁴⁷ After laser-micro-annealing, an enhancement of the integrated photoluminescence intensity is observed related to $V_{\text{eff, LMA}} > V_{\text{eff, w/o LMA}}$. A reduction of defect layer depth ($\text{depth}_{\text{def}}$) from $\sim 17 \text{ nm}$ to $\sim 5 \text{ nm}$ was determined. Hence, the origin of the observed enhanced integrated photoluminescence intensity is in good agreement with the simplified model presented.

For the sake of comparison, current–voltage measurements were performed on single non-locally annealed and locally annealed nano-LED structures using different annealing conditions I and II (laser power: $\sim 0.8 \text{ kW/cm}^2$ and annealing time: 2 s and 4 s, respectively).

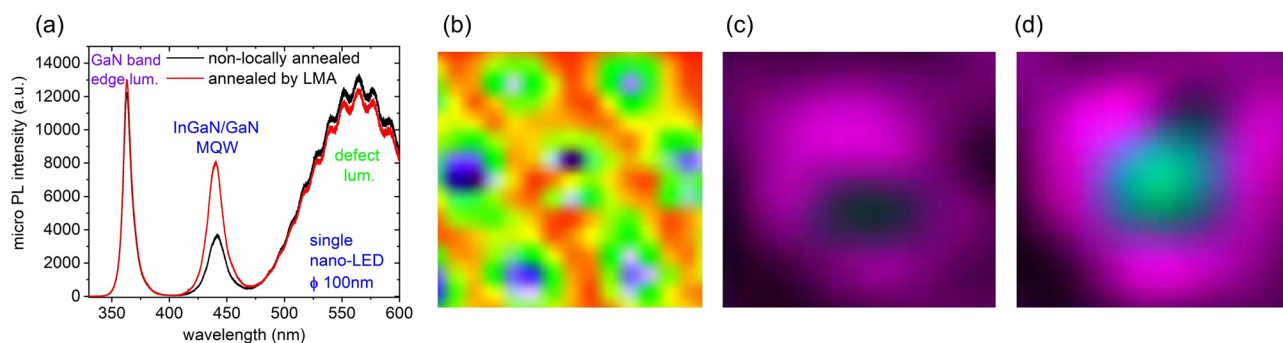


FIG. 2. Micro-photoluminescence measurements (a) performed on a single nano-LED (diameter $\sim 100 \text{ nm}$) before and after LMA. A significant increase (more than 100%) is observed in the “blue” luminescence range centered around 440–445 nm MQW. (b) Micro-PL mapping: from the single nano-LEDs in the array—the etching process is responsible for the suppression of radiative recombination from the MQW region: blue color with inhomogeneous intensity corresponds to $\sim 440\text{--}445 \text{ nm}$ of the emission maxima in the PL spectra, green–yellow and red to ($\sim 540\text{--}600 \text{ nm}$) at the individually measured points. Comparison of (c) a non-locally annealed vs (d) an LMA conditioned nano-LED: a significant increase in photoluminescence intensity (blue/turquoise color) from the central region of the single nano-LED is observed in the $\sim 440\text{--}445 \text{ nm}$ emission wavelength range and a moderate increase is found in GaN band edge luminescence at $\sim 362.8 \text{ nm}$ (3.418 eV) corresponding to the “pink” color after LMA conditioning. Note that colors chosen for these micro-PL graphics serve only as a guide to the eye to help understand the distribution of emission from the region with the MQW structures and the surrounding etched regions.

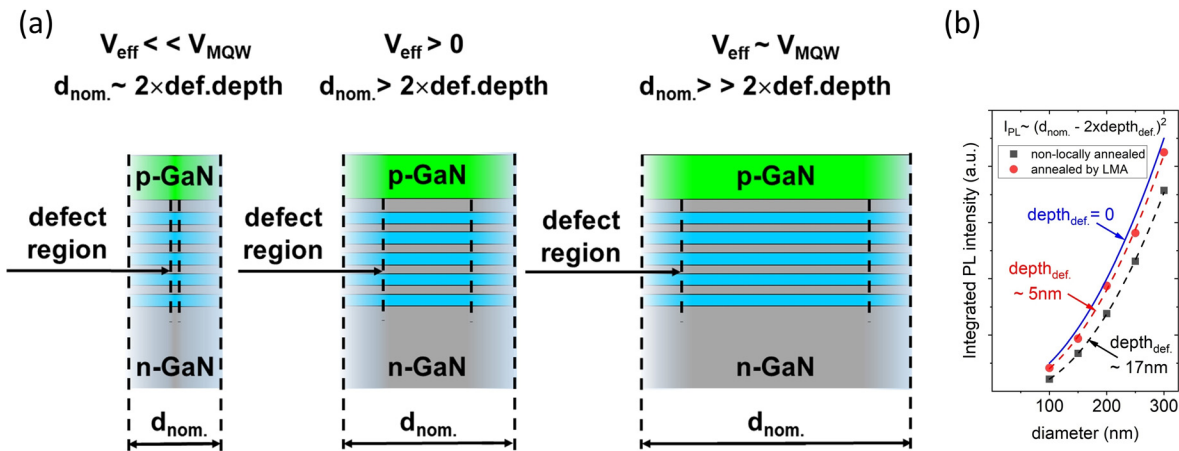


FIG. 3. (a) Simple model showing the effect of the defect layer depth on the virtual equivalent of the effective volume (V_{eff}): the effect is the larger the smaller the nominal diameter $d_{nom.}$. (b) Integrated photoluminescence intensity normalized to the as-grown MQW (parent) structure as a function of $d_{nom.}$ for different nano-LED diameters. After laser-micro-annealing (LMA), an enhancement of the integrated photoluminescence intensity is observed ($V_{eff, LMA} > V_{eff, w/o LMA}$). A reduction of defect layer depth ($depth_{def.}$) from $\sim 17 \text{ nm}$ to $\sim 5 \text{ nm}$ was determined.

Representative curves for the identical nano-LED structure before and after LMA are shown in Fig. 4(a) after 1 min of operation. The current increase after applying LMA and at 5 V bias is ~ 3.7 times higher for the condition II annealed nano-LED. Figure 4(b) presents an example of a micro-EL mapping of the nano-LED array in which ensembles of individual nano-LEDs were locally annealed with conditions I and II as presented in the current-voltage characteristic [Fig. 4(a)] reaching the intended EL intensities E1 and E2. The locally conditioned nano-LEDs' intensity increases with respect to that of their non-locally annealed counterparts (E0) according to the LMA-process conditions used. These results could be attributed to the Ohmic contact improvement as well as to a curing of defects in the nano-LEDs. It also demonstrates the potential of the LMA conditioning procedure, which can be applied to intentionally reach the appropriate optical properties of nano-LED hybrid photon sources^{5,7} and nano-LEDs in arrays for

single photon-assisted lithography, on the one hand,²³ and especially for creating patterns of optical gate sources functionally arranged for future logical circuits based on transistor devices⁴⁸ currently under development, on the other hand.

Micro-EL studies of a nano-LED with a diameter of $\sim 100 \text{ nm}$ were performed at 5 V bias voltage before and after the local conditioning was carried out. The ultimate reliability test for the nano-LEDs is the study of their electroluminescence under continuous wave (cw) operation⁴⁹ for 5000 h. Spectra recorded at the beginning of the reliability study (time 1 min) are presented in Fig. 5(a). The maximum of the intensity is a factor of close to four lower for the non-locally annealed nano-LED. For both nano-LEDs, a sudden and large intensity drop is observed within the first 100 h of operation and a slower intensity decrease up to 5000 h of operation thereafter [Fig. 5(b)]. This corresponds to an intensity reduction of $\sim 9\%$ and $\sim 20\%$ within the first 100 h and by $\sim 15\%$ and $\sim 50\%$ in total after 5000 h for the locally conditioned and non-locally annealed nano-LEDs, respectively. It is apparent that the stability and reliability of the nano-LEDs are higher, when LMA conditioning is applied. The difference in EL-intensity increases from close to four to more than six.

At last, Raman spectroscopy was performed on the nano-LEDs under 5 V bias voltage. It is well known that besides changes in chemical specific information in materials such as bonding, environment, and strain/stress, this method can be employed for thermography and, therefore, to discern possible differences of the device temperatures during operation.^{50–53} In GaN, the line position of the Raman shift of the E_2^H mode⁵⁴ would be an indication of the difference in device temperature during operation: the increase in the position of the Raman shift is related to a lower temperature in the nano-LED device. A comparison of the Raman spectra of the nano-LEDs in operation which were not additionally treated with LMA [i.e., those only non-locally (thermally) annealed] with those which were locally annealed [Fig. 5(c)] disclosed that the shift of the E_2^H mode increases from $\sim 570 \text{ cm}^{-1}$ to $\sim 571.3 \text{ cm}^{-1}$ after local conditioning. The increase could relate to a reduction of the work temperature of up to $\sim 60 \text{ K}$ (Refs. 51, 52, and 55)

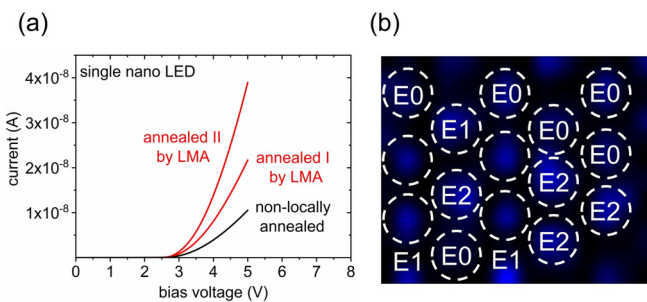


FIG. 4. (a) Current-voltage characteristic behavior for three stages of an annealed single nano-LED. Significant Ohmic contact improvement is discerned: more than three times higher currents at 5 V bias voltage were evaluated after the LMA procedure II was applied in comparison to the non-locally annealed structure. (b) Micro-EL performed on nano-LEDs in an array with three different annealing conditions: non-locally annealed E0 and locally E1 and E2 annealed [with conditions I and II, see (a)]. The LEDs' EL intensity becomes higher according to the LMA process carried out.

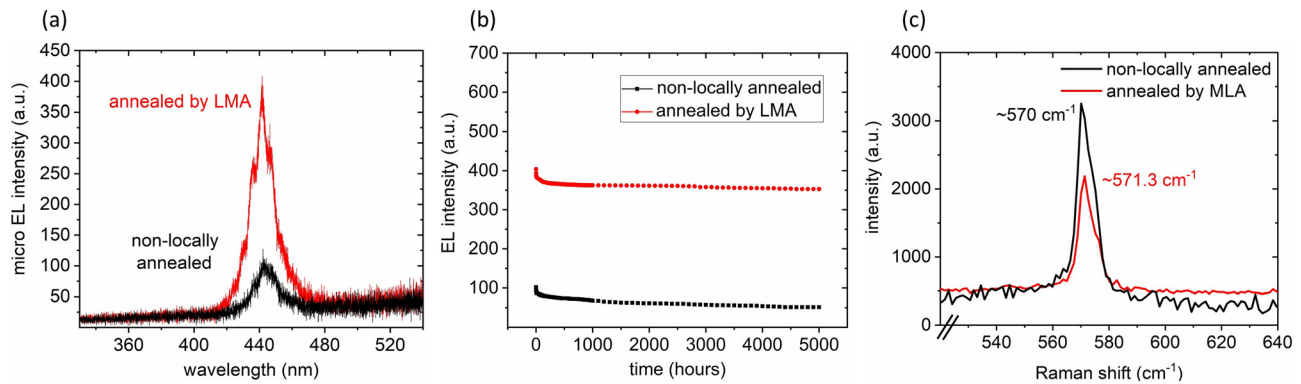


FIG. 5. (a) Micro-EL measurements performed on single nano-LEDs (diameter ~ 100 nm) at 5 V bias voltage, (b) reliability/long-term micro-EL measurements performed on nano-LED devices during 5000 h under cw operation testing mode, and (c) Raman measurements at different work temperatures performed on single nano-LEDs (diameter ~ 100 nm) before and after laser-micro-annealing (condition II). A significant EL-intensity increase and an improved emission reliability operation are observed. The line position of the Raman shift of the E_2^H mode increases for the locally LMA conditioned nano-LED, indicating a reduction of work temperature after LMA conditioning.

after annealing. This results in a higher efficiency of the nano-LED and is advantageous for its stable and reliable operation.

In conclusion, a laser-micro-annealing (LMA) technology was introduced and developed for group III-nitride-based nano-light emitting diodes (LEDs) and applied locally to the Ohmic Ni/Au contacts to p-GaN. The charge transport and light emission of the annealed devices were determined and compared to their non-LMA conditioned counterparts. PL studies revealed an increase in radiative recombination by more than a factor of two, which is attributed to a curing of RIE-induced defects. The enhancement of nano-LED properties is in good agreement with a simple model introduced based on the reduction of the defect layer depth by the LMA process. A decrease from ~ 17 nm to ~ 5 nm, i.e., an increase in effective nano-LED MQW volume contributing to radiative recombination, was determined. By applying appropriate annealing conditions, different nano-LED characteristics can be achieved intentionally. An increase in work currents up to 40 nA at 5 V bias and a high electroluminescence and output optical power up to 150 nW in the ~ 440 – 445 nm emission wavelength range corresponding to $\sim 75\%$ overall efficiency were achieved. The conditioned nano-LEDs exhibit a reduction of work temperature of up to ~ 60 K and an improved long term stability under cw operation compared to their non-LMA conditioned counterparts. Laser-micro-annealing conditioning of nano-LEDs results in the enhancement of their performance and is the key to stable and reliable nano-LED operation.

AUTHORS' CONTRIBUTIONS

All authors contributed equally to this work.

Z.S. would like to thank the Ministry of Education Youth and Sports (MEYS) of the Czech Republic for supporting this work by the Project No. LTAUSA19034.

DATA AVAILABILITY

The data that support the findings of this study are available from the corresponding author upon reasonable request.

REFERENCES

- ¹H. Amano, in *III-Nitride Based Light Emitting Diodes and Applications*, Topics in Applied Physics, edited by T. Y. Seong, J. Han, H. Amano, and H. Morkoc (Springer Nature, Singapore, 2017), pp. 1–9.
- ²Y. Li, F. Qian, J. Xiang, and C. M. Lieber, *Mater. Today* **9**, 18 (2006).
- ³V. M. Agranovich, Y. N. Gartstein, and M. Litinskaya, *Chem. Rev.* **111**, 5179 (2011).
- ⁴Y. Wang, X. Wang, B. Zhu, Z. Shi, J. Yuan, X. Gao, Y. Liu, X. Sun, D. Li, and H. Amano, *Light* **7**, 83 (2018).
- ⁵H. Hardtdegen and M. Mikulics, in *2016 11th International Conference on Advanced Semiconductor Devices and Microsystems* (IEEE, 2016), pp. 27–32.
- ⁶H. Haug and S. W. Koch, *Quantum Theory of the Optical and Electronic Properties of Semiconductors* (World Scientific, 2009).
- ⁷M. Mikulics, Y. C. Arango, A. Winden, R. Adam, A. Hardtdegen, D. Grützacher, E. Plinski, D. Gregušová, J. Novák, P. Kordoš, A. Moonshiram, M. Marso, Z. Sofer, H. Lüth, and H. Hardtdegen, *Appl. Phys. Lett.* **108**, 061107 (2016).
- ⁸F. M. Steranka, J. Bhat, D. Collins, L. Cook, M. G. Craford, R. Fletcher, N. Gardner, P. Grillot, W. Goetz, M. Keuper, R. Khare, A. Kim, M. Krames, G. Harbers, M. Ludowise, P. S. Martin, M. Misra, G. Mueller, R. Mueller-Mach, S. Rudaz, Y.-C. Shen, D. Steigerwald, S. Stockman, S. Subramanya, T. Trotter, and J. J. Wierer, *Phys. Status Solidi* **194**, 380 (2002).
- ⁹A. Prasad, L. Du, M. Zubair, S. Subedi, A. Ullah, and M. S. Roopesh, *Food Eng. Rev.* **12**, 268 (2020).
- ¹⁰Y. Nanishi, *Nat. Photonics* **8**, 884 (2014).
- ¹¹Z. Gong, S. Jin, Y. Chen, J. McKendry, D. Massoubre, I. M. Watson, E. Gu, and M. D. Dawson, *J. Appl. Phys.* **107**, 013103 (2010).
- ¹²M. Malinverni, D. Martin, and N. Grandjean, *Appl. Phys. Lett.* **107**, 051107 (2015).
- ¹³D. Hwang, A. J. Mughal, M. S. Wong, A. I. Alhassan, S. Nakamura, and S. P. DenBaars, *Appl. Phys. Express* **11**, 012102 (2018).
- ¹⁴Z. Y. Fan, J. Y. Lin, and H. X. Jiang, *J. Phys. D* **41**, 094001 (2008).
- ¹⁵N. Franch, J. Canals, V. Moro, O. Alonso, S. Moreno, A. Vilà, J. D. Prades, J. Gülink, H. S. Wasisto, A. Waag, and Á. Diéguez, in *Novel Optical Systems, Methods, and Applications XXII*, edited by C. F. Hahlweg and J. R. Mulley (SPIE, 2019), p. 23.
- ¹⁶J. J. Wierer and N. Tansu, *Laser Photonics Rev.* **13**, 1900141 (2019).
- ¹⁷F. Templier, *J. Soc. Inf. Disp.* **24**, 669 (2016).
- ¹⁸H. S. Wasisto, J. D. Prades, J. Gülink, and A. Waag, *Appl. Phys. Rev.* **6**, 041315 (2019).
- ¹⁹R. Ley, L. Chan, P. Shapturenka, M. Wong, S. DenBaars, and M. Gordon, *Opt. Express* **27**, 30081 (2019).
- ²⁰L. Chan, P. Shapturenka, C. D. Pynn, T. Margalith, S. P. DenBaars, and M. J. Gordon, *Appl. Phys. Lett.* **117**, 021104 (2020).

- ²¹S. Bharadwaj, K. Lee, K. Nomoto, A. Hickman, L. van Deurzen, V. Protasenko, H. G. Xing, and D. Jena, *Appl. Phys. Lett.* **117**, 031107 (2020).
- ²²M. Mikulics, A. Winden, M. Marso, A. Moonshiram, H. Lüth, D. Grützmacher, and H. Hardtdegen, *Appl. Phys. Lett.* **109**, 041103 (2016).
- ²³M. Mikulics and H. Hardtdegen, *Nanotechnology* **26**, 185302 (2015).
- ²⁴A. Di Vito, A. Pecchia, A. Di Carlo, and M. Auf der Maur, *J. Appl. Phys.* **128**, 041102 (2020).
- ²⁵J. Moers, M. Mikulics, M. Marso, S. Trellenkamp, Z. Sofer, D. Grützmacher, and H. Hardtdegen, in *2016 11th International Conference on Advanced Semiconductor Devices and Microsystems* (IEEE, 2016), pp. 81–84.
- ²⁶R. T. Ley, J. M. Smith, M. S. Wong, T. Margalith, S. Nakamura, S. P. DenBaars, and M. J. Gordon, *Appl. Phys. Lett.* **116**, 251104 (2020).
- ²⁷G. K. Celler, J. M. Poate, and L. C. Kimerling, *Appl. Phys. Lett.* **32**, 464 (1978).
- ²⁸R. T. Young, C. W. White, G. J. Clark, J. Narayan, W. H. Christie, M. Murakami, P. W. King, and S. D. Kramer, *Appl. Phys. Lett.* **32**, 139 (1978).
- ²⁹C. Lee, P. Srisungsitthisunti, S. Park, S. Kim, X. Xu, K. Roy, D. B. Janes, C. Zhou, S. Ju, and M. Qi, *ACS Nano* **5**, 1095 (2011).
- ³⁰H. Kwon, W. Choi, D. Lee, Y. Lee, J. Kwon, B. Yoo, C. P. Grigoropoulos, and S. Kim, *Nano Res.* **7**, 1137 (2014).
- ³¹J. Ha, B. J. Lee, D. J. Hwang, and D. Kim, *RSC Adv.* **6**, 86232 (2016).
- ³²T. Hashizume, S. Kaneki, T. Oyobiki, Y. Ando, S. Sasaki, and K. Nishiguchi, *Appl. Phys. Express* **11**, 124102 (2018).
- ³³Y. Ando, S. Kaneki, and T. Hashizume, *Appl. Phys. Express* **12**, 024002 (2019).
- ³⁴M. Mikulics, J. G. Lu, L. Huang, P. L. Tse, J. Z. Zhang, J. Mayer, and H. Hardtdegen, *FlatChem* **21**, 100164 (2020).
- ³⁵T. C. Shen, *J. Vac. Sci. Technol. B* **10**, 2113 (1992).
- ³⁶J. O. Song, J.-S. Ha, and T.-Y. Seong, *IEEE Trans. Electron Devices* **57**, 42 (2010).
- ³⁷A. Macková, P. Malinský, A. Jágerová, Z. Sofer, K. Klímová, D. Sedmidubský, M. Mikulics, R. Böttger, and S. Akhmadaliev, *Surf. Coat. Technol.* **355**, 22 (2018).
- ³⁸I. Kim, P. Kivisaari, J. Oksanen, and S. Suihkonen, *Materials* **10**, 1421 (2017).
- ³⁹Y. S. Cho, H. Hardtdegen, N. Kaluza, N. Thillosen, R. Steins, Z. Sofer, and H. Lüth, *Phys. Status Solidi* **3**, 1408 (2006).
- ⁴⁰H. Hardtdegen, M. Pristovsek, H. Menhal, J.-T. Zettler, W. Richter, and D. Schmitz, *J. Cryst. Growth* **195**, 211 (1998).
- ⁴¹Y. C. Lin, S. J. Chang, Y. K. Su, T. Y. Tsai, C. S. Chang, S. C. Shei, C. W. Kuo, and S. C. Chen, *Solid-State Electron.* **47**, 849 (2003).
- ⁴²S. Nakamura, T. Mukai, M. Senoh, and N. Iwasa, *Jpn. J. Appl. Phys., Part 2* **31**, L139 (1992).
- ⁴³J. Hsieh, J. Hwang, H. Hwang, O. Breitschädel, and H. Schweizer, *Appl. Surf. Sci.* **175-176**, 450 (2001).
- ⁴⁴M. Mikulics, H. Hardtdegen, D. Gregušová, Z. Sofer, P. Šimek, S. Trellenkamp, D. Grützmacher, H. Lüth, P. Kordoš, and M. Marso, *Semicond. Sci. Technol.* **27**, 105008 (2012).
- ⁴⁵T. Sameshima, M. Hasumi, and T. Mizuno, *Appl. Surf. Sci.* **336**, 73 (2015).
- ⁴⁶H.-Y. Ryu, D.-S. Shin, and J.-I. Shim, *Appl. Phys. Lett.* **100**, 131109 (2012).
- ⁴⁷Y.-J. Lin and Y.-L. Chu, *J. Appl. Phys.* **97**, 104904 (2005).
- ⁴⁸M. Mikulics and H. H. Hardtdegen, *FlatChem* **23**, 100186 (2020).
- ⁴⁹J. Ruschel, J. Glaab, F. Mahler, T. Kolbe, S. Einfeldt, and J. W. Tomm, *Appl. Phys. Lett.* **117**, 121104 (2020).
- ⁵⁰M. Kuball, J. W. Pomeroy, R. Simms, G. J. Riedel, H. Ji, A. Sarua, M. J. Uren, and T. Martin, in *2007 IEEE Compound Semiconductor Integrated Circuits Symposium* (IEEE, 2007), pp. 1–4.
- ⁵¹M. S. Liu, L. a Bursill, S. Prawer, K. W. Nugent, Y. Z. Tong, and G. Y. Zhang, *Appl. Phys. Lett.* **74**, 3125 (1999).
- ⁵²J. Senawiratne, Y. Li, M. Zhu, Y. Xia, W. Zhao, T. Detchprohm, A. Chatterjee, J. L. Plawsky, and C. Wetzel, *J. Electron. Mater.* **37**, 607 (2008).
- ⁵³J. Zhang, T. Shih, Y. Lu, H. Merlitz, R. Ru-Gin Chang, and Z. Chen, *Sci. Rep.* **6**, 19539 (2016).
- ⁵⁴H. Harima, *J. Phys.* **14**, R967 (2002).
- ⁵⁵M. Kuball, *Surf. Interface Anal.* **31**, 987 (2001).